Solar Phys (2018) 293:136
https://doi.org/10.1007/s11207-018-1354-x

First Analysis of Ground-Level Enhancement (GLE) 72 on 10 September 2017: Spectral and Anisotropy Characteristics

A. Mishev[1,2] · I. Usoskin[1,2] · O. Raukunen[3] · M. Paassilta[3] · E. Valtonen[3] · L. Kocharov[2] · R. Vainio[3]

Received: 7 November 2017 / Accepted: 3 September 2018

Abstract Using data obtained with neutron monitors and space-borne instruments, we analyzed the second ground-level enhancement (GLE) of Solar Cycle 24, namely the event of 10 September 2017 (GLE 72), and derived the spectral and angular characteristics of associated GLE particles. We employed a new neutron-monitor yield function and a recently proposed model based on an optimization procedure. The method consists of simulating particle propagation in a model magnetosphere in order to derive the cutoff rigidity and neutron-monitor asymptotic directions. Subsequently, the rigidity spectrum and anisotropy of GLE particles are obtained in their dynamical evolution during the event on the basis of an inverse-problem solution. The derived angular distribution and spectra are discussed briefly.

Keywords Solar cosmic rays · Energetic particles · Protons

1. Introduction

A detailed study of solar energetic particle (SEP) events provides an important basis for understanding their acceleration and propagation in interplanetary space (Debrunner *et al.*, 1988; Lockwood, Debrunner, and Flückiger, 1990; Kallenrode, Cliver, and Wibberenz, 1992; Reames, 1999; Drake *et al.*, 2009; Tylka and Dietrich, 2009; Li *et al.*, 2012; Vainio *et al.*, 2013; Gopalswamy *et al.*, 2014; Kocharov *et al.*, 2017; Vainio *et al.*, 2017). Energetic and sporadic solar flares and coronal mass ejections (CMEs) can produce SEPs (*e.g.* Reames, 1999; Cliver, Kahler, and Reames, 2004; Aschwanden, 2012; Reames, 2013; Desai and Giacalone, 2016, and references therein). The maximum energy of SEPs is typically

✉ A.L. Mishev
alexander.mishev@oulu.fi

I.G. Usoskin
ilya.usoskin@oulu.fi

1 Space Climate Research Unit, University of Oulu, Oulu, Finland

2 Sodankylä Geophysical Observatory (Oulu unit), University of Oulu, Oulu, Finland

3 Department of Physics and Astronomy, University of Turku, Turku, Finland

Published online: 04 October 2018

several MeV nucleon^{-1}, rarely exceeding 100 MeV nucleon^{-1}. However, in some cases, the SEP energy reaches several GeV nucleon^{-1}. While lower energy SEPs are absorbed in the atmosphere, those with energy above 300 – 400 MeV nucleon^{-1} can generate an atmospheric shower, *i.e.* a complicated nuclear-electromagnetic-muon cascade consisting of a large number of secondary particles that can reach the ground and eventually be registered by ground-based detectors, *e.g.* neutron monitors (NMs) (*e.g.* Dorman, 2004, and references therein). The probability of occurrence of a high-energy SEP event is higher during the maximum and declining phase of the solar activity cycle (*e.g.* Shea and Smart, 1990). This particular class of events is known as ground-level enhancements (GLEs).

Such events are usually studied using the worldwide NM network (Simpson, Fonger, and Treiman, 1953; Hatton, 1971; Bieber and Evenson, 1995; Stoker, Dorman, and Clem, 2000; Mavromichalaki *et al.*, 2011; Gopalswamy *et al.*, 2012, 2014; Moraal and McCracken, 2012; Papaioannou *et al.*, 2014). The distribution of NMs at different geographic regions allows obtaining an exhaustive record of cosmic rays in space, because their intensity is not uniform in the vicinity of Earth (Bieber and Evenson, 1995; Mavromichalaki *et al.*, 2011). This fact plays an important role for GLE analysis, since an essential anisotropic part, normally during the event onset, is observed (Vashenyuk *et al.*, 2006; Bütikofer *et al.*, 2009; Mishev and Usoskin, 2016a). The full list of NMs used for the analysis of GLE 72 on 10 September 2017, with the corresponding abbreviations, cutoff rigidities, and altitudes, is given in Table 1.

The first ten days of September 2017 were characterized by intense solar activity. During this period, several X-class flares and CMEs were produced. The GLE 72 on 10 September 2017 was related to an X8.2 solar flare, the climax of a series of flares from Active Region 2673. It peaked at 16:06 UT, leading to a gradual SEP event measured by spacecraft up to proton energies exceeding 700 MeV nucleon^{-1} (Figure 1) and to a very fast CME erupting over the western limb (Figure 2). The CME was first observed in the *Solar and Heliospheric Observatory* (SOHO)/*Large Angle and Spectrometric Coronagraph* LASCO-C2 field of view at 16:00:07 UT. The initial speed of the CME was very high, 3620 km s^{-1}, as measured from the leading edge of the structure at position angle 270°, *i.e.* to the west. The CME drove a shock front through the corona, whose flanks were traced in the *Atmospheric Imaging Assembly* (AIA) of the *Solar Dynamics Observatory* (SDO) spacecraft (Lemen *et al.*, 2012), and whose nose was visible as a fainter structure in front of the brightest part of the CME.

The GLE onset was observed by several NM stations at about 16:15 UT (*e.g.* FSMT and INVK with statistically significant count rate increase), and the corresponding alert signal was revealed after 17:00 (Souvatzoglou *et al.*, 2014). However, a statistically significant and high enough signal, which allows deriving the spectral and angular characteristics of SEPs with sufficient precision, was observed at 16:30 UT, *i.e.* only 15 minutes after the onset of the GLE in the data of the first NM station (see Sections 2 and 3). The strongest NM count rate increase were observed at DOMC/DOMB (10 – 15%, Figure 3a), SOPO/SOPB (5 – 8%, Figure 3a), and FSMT ($\approx$6%, Figure 3f) compared to the pre-increase levels; see details in Figure 3. The count-rate increase at FSMT was steeper than at other stations, which recorded gradual increases. Here DOMB and SOPB correspond to the lead-free NMs at Dome C and the South Pole stations, respectively. The event was characterized by a typical gradual increase, a relatively hard rigidity spectrum, and a strong to moderate anisotropy during the event onset, which rapidly decreases and resulted in a nearly isotropic flux. Similarly to some other events, it occurred during the recovery phase of a Forbush decrease, which is explicitly considered in our analysis. The background due to galactic cosmic rays (GCRs) is averaged over two hours before the event onset, and therefore we accounted for the corresponding

Table 1 Neutron monitors with corresponding cutoff rigidities, geographic coordinates, and altitudes above sea level used for the analysis of GLE 72.

Station	Latitude [deg]	Longitude [deg]	P_c [GV]	Altitude [m]
Alma Aty (AATY)	43.25	76.92	6.67	3340
Apatity (APTY)	67.55	33.33	0.48	177
Athens (ATHN)	37.98	23.78	8.42	260
Baksan (BKSN)	43.28	42.69	5.6	1700
Dome C (DOMC)	−75.06	123.20	0.1	3233
Dourbes (DRBS)	50.1	4.6	3.34	225
Fort Smith (FSMT)	60.02	248.07	0.25	0
Inuvik (INVK)	68.35	226.28	0.16	21
Irkutsk (IRKT)	52.58	104.02	3.23	435
Jang Bogo(JNBG)	−74.37	164.13	0.1	29
Jungfraujoch (JUNG)	46.55	7.98	4.46	3476
Kerguelen (KERG)	−49.35	70.25	1.01	33
Lomnicky Štit (LMKS)	49.2	20.22	3.72	2634
Magadan (MGDN)	60.12	151.02	1.84	220
Mawson (MWSN)	−67.6	62.88	0.22	0
Mexico city (MXCO)	19.33	260.8	7.59	2274
Moscow (MOSC)	55.47	37.32	2.13	200
Nain (NAIN)	56.55	298.32	0.28	0
Newark (NWRK)	39.70	284.30	1.97	50
Oulu (OULU)	65.05	25.47	0.69	15
Peawanuck (PWNK)	54.98	274.56	0.16	52
Potchefstroom (PTFM)	−26.7	27.09	6.98	1351
Rome (ROME)	41.9	12.52	6.11	60
South Pole (SOPO)	−90.00	0.0	0.01	2820
Terre Adelie (TERA)	−66.67	140.02	0	45
Thule (THUL)	76.60	291.2	0.1	260
Tixie Bay (TXBY)	71.60	128.90	0.53	0

variations in the count rates of each NM for an exact computation of the background. We here analyze this event using five-minute-integrated NM data retrieved from the neutron-monitor database NMDB (www.nmdb.eu/: *e.g.* Mavromichalaki *et al.*, 2011), available also at the international GLE database (gle.oulu.fi/#/).

2. Modeling the Neutron Monitor Response

We employed a method similar to the method reported by Shea and Smart (1982), Humble *et al.* (1991), Cramp *et al.* (1997), Bombardieri *et al.* (2006), and Vashenyuk *et al.* (2006, 2008). A detailed description of the method is given elsewhere (Mishev, Kocharov, and Usoskin, 2014; Mishev and Usoskin, 2016a; Mishev, Usoskin, and Kocharov, 2017; Mishev, Poluianov, and Usoskin, 2017). The method implies modeling the NM response using an initial guess, similarly to Mishev and Usoskin (2016b), Kocharov *et al.* (2017), and/or to Cramp, Humble, and Duldig (1995) and includes an optimization procedure over a selected

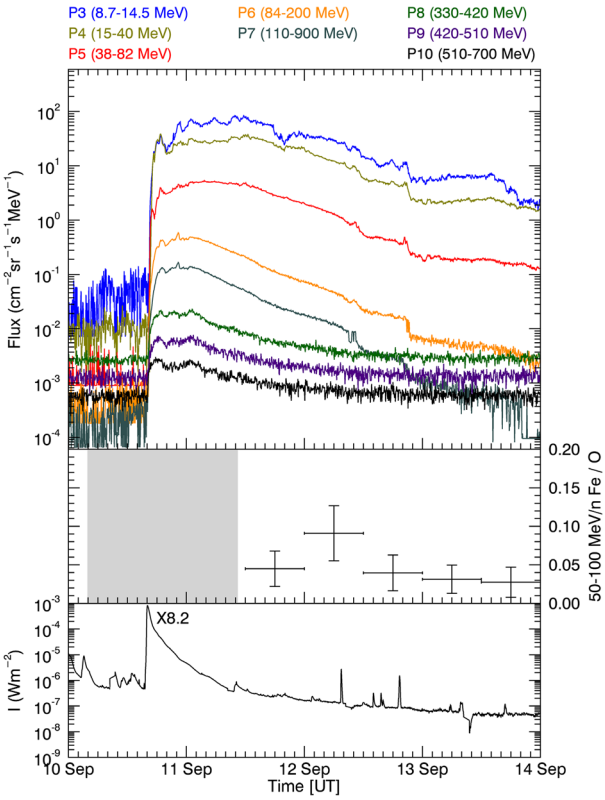

Figure 1 10 September 2017 SEP event and related gradual soft X-ray flare as observed by GOES and SOHO/ERNE. The *top panel* shows the proton fluxes measured by GOES, the *middle panel* shows the Fe/O ratio at 50 – 100 MeV nucleon^{-1} measured by SOHO/ERNE, and the *bottom panel* shows the soft X-ray intensity measured by GOES. Note that SOHO/ERNE had a data gap at the beginning of the SEP event, indicated by the *gray area* in the corresponding panel.

space of unknowns describing SEP characteristics. For a good convergence of the optimization, we need about $2(n-1)$ NM stations with non-null response, where n is the number of unknowns (*e.g.* Himmelblau, 1972). However, our method allows us to derive a robust solution even in the case of relatively weak recorded NM increases on the basis of a specific numeric procedure: a variable regularization (*e.g.* Tikhonov *et al.*, 1995; Mishev, Poluianov, and Usoskin, 2017).

We used a newly computed NM yield function (Mishev, Usoskin, and Kovaltsov, 2013) that agrees well with experiments and recent modeling (Gil *et al.*, 2015; Mangeard *et al.*, 2016). We reduced the model uncertainties related to the normalization of high-altitude NMs to sea level by employing, when possible, a yield function corresponding to the proper altitude of the NMs above sea level (*e.g.* Mishev, Usoskin, and Kovaltsov, 2016) and appropriate scaling of mini-NM to a standard 6NM64 (Caballero-Lopez, 2016; Lara, Borgazzi, and Caballero-Lopez, 2016).

In our model we can use as an approximation a modified power-law or an exponential rigidity spectrum similarly to Cramp *et al.* (1997) and Vashenyuk *et al.* (2008). The rigidity spectrum of SEPs described by a modified power law is given by the expression

$$J_{||}(P) = J_0 P^{-(\gamma+\delta\gamma(P-1))}, \tag{1}$$

where $J_{||}(P)$ denotes the flux of particles with rigidity P, which arrive from the Sun along the axis of symmetry identified by geographic latitude Ψ and longitude Λ. The spectrum is described by a power-law exponent $[\gamma]$ and the rate of the spectrum steepening $[\delta\gamma]$.

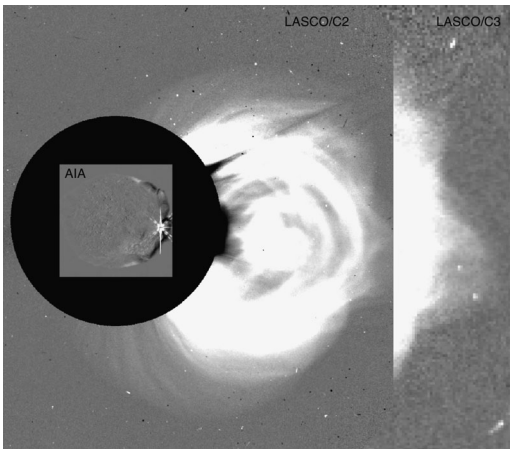

Figure 2 SOL 2017-09-10T16:00:07 CME as observed by SOHO/LASCO and SDO/AIA. The observation times of AIA and LASCO-C2 are 16:12:08 and 16:12:48, respectively. AIA observations are shown in 24-minute running-difference images and the LASCO observations in 12-minute (or the best possible) running-difference images. The C3 image shows the CME only 6 minutes later than the C2 image, indicating how exceptionally fast the CME was. All frames are centered in the same way and have the same scale. The image was created using Helioviewer (www.helioviewer.org).

Accordingly, the exponential rigidity spectrum is given by

$$J_{||}(P) = J_0 \exp(-P/P_0), \tag{2}$$

where P_0 is a characteristic proton rigidity.

The pitch-angle distribution (PAD) in all cases was modeled as a superposition of two Gaussians:

$$G\big(\alpha(P)\big) \sim \exp\big(-\alpha^2/\sigma_1^2\big) + B\exp\big(-(\alpha-\pi)^2/\sigma_2^2\big), \tag{3}$$

where α is the pitch angle, σ_1 and σ_2 quantify the width of the pitch-angle distribution, and B describes the amount of particle flux arriving from the anti-Sun direction. This allows us to consider a bidirectional particle flow.

The optimization was performed by minimizing the squared sum of differences between the modeled and measured NM responses employing the Levenberg–Marquardt method (Levenberg, 1944; Marquardt, 1963) with variable regularization (Tikhonov *et al.*, 1995), similarly to Mavrodiev, Mishev, and Stamenov (2004). We assessed the goodness of fit on the basis of several criteria. The general criterion $\mathcal{D}$, *i.e.* the residual (Equation 4), is according to Himmelblau (1972) and Dennis and Schnabel (1996):

$$\mathcal{D} = \frac{\sqrt{\sum_{i=1}^{m}[(\frac{\Delta N_i}{N_i})_{\text{mod.}} - (\frac{\Delta N_i}{N_i})_{\text{meas.}}]^2}}{\sum_{i=1}^{m}(\frac{\Delta N_i}{N_i})_{\text{meas.}}}. \tag{4}$$

According to our experience, a good convergence of the optimization process and a robust solution are reached for $\mathcal{D} \leq 5\%$, similarly to Vashenyuk *et al.* (2006) and Mishev and Usoskin (2016a). Normally, $\mathcal{D}$ is roughly 5% for strong events and $\approx 10-15\%$ for weak events such as GLE 72 (*e.g.* Mishev, Usoskin, and Kocharov, 2017; Mishev, Poluianov, and Usoskin, 2017). Therefore, we used additional criteria: the relative difference between the

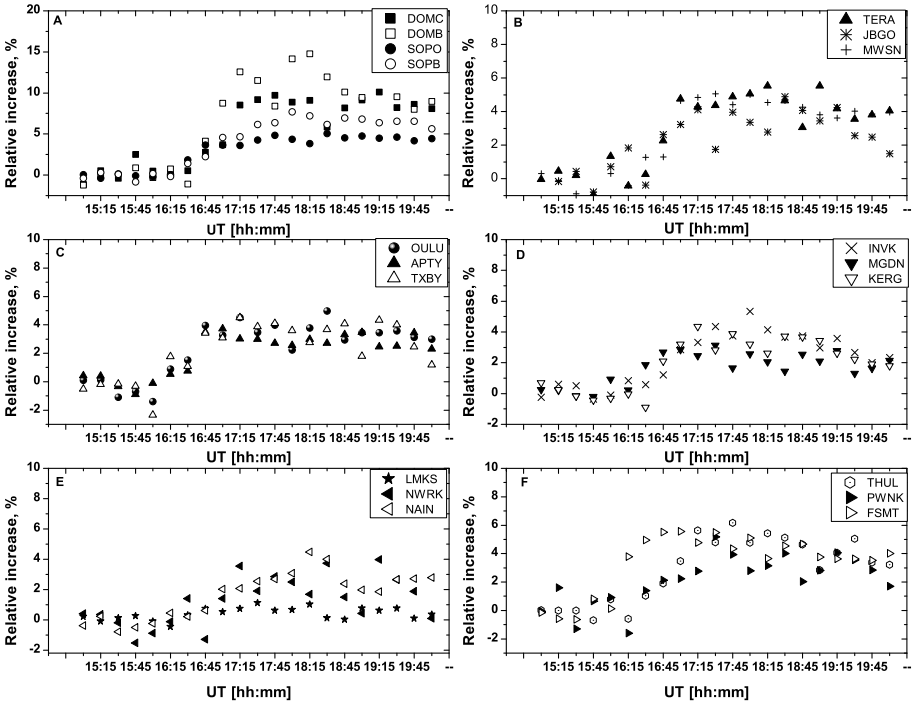

Figure 3 Count-rate variation of NMs with a statistically significant increase during GLE 72 on 10 September 2017.

observed and calculated relative NM count-rate increases should be about 10 – 20% for each station and the residuals should have a nearly symmetric distribution, *viz.* the number of NMs under- and/or overestimating the count rate must be roughly equal (*e.g.* Himmelblau, 1972).

We modeled the SEP propagation in the geomagnetosphere that we used to compute the cutoff rigidities and asymptotic directions of NMs (Cooke *et al.*, 1991) with the MAGNETOCOSMICS code (Desorgher *et al.*, 2005), using the International Geomagnetic Reference Field (IGRF) geomagnetic model (epoch 2015) as the internal-field model (Langel, 1987) and the Tsyganenko 89 model as the external field (Tsyganenko, 1989). This combination provides a straightforward and precise modeling of the SEP propagation in the Earth's magnetosphere (Kudela and Usoskin, 2004; Kudela, Bučik, and Bobik, 2008; Nevalainen, Usoskin, and Mishev, 2013).

3. Results of the Analysis

We studied different cases, assumed in our model, of spectral and PAD functional shapes: modified power-law or exponential rigidity spectra of SEPs, and single or double Gaussian PAD, which encompass all of the possibilities in the model (Equations 1 – 3). An example of several computed asymptotic directions that we used for the analysis of GLE 72 is presented in Figure 4. Here we plot the asymptotic directions in the rigidity range from 1 to 5 GV (for DOMC and SOPO from 0.7 to 5 GV, respectively) in order to show the range of maximum

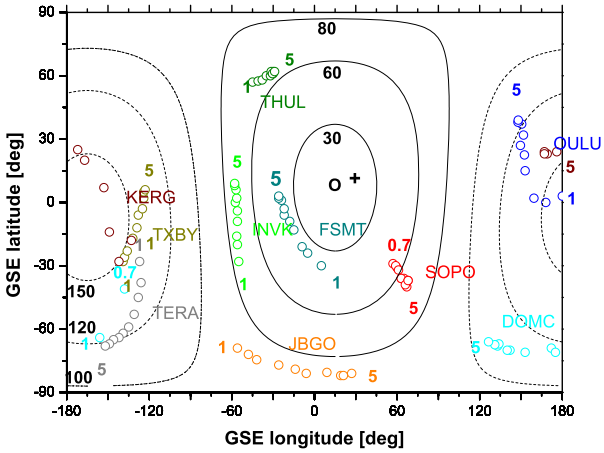

Figure 4 Asymptotic directions of several NM stations during the GLE 72 event on 10 September 2017 at 16:45 UT. The *colored lines* and numbers indicate the NM stations and asymptotic directions (abbreviations given in Table 1). The *small oval* depicts the derived apparent source position, the cross depicts the IMF according to ACE satellite measurements. The lines of equal pitch angles relative to the derived anisotropy axis are plotted for 30°, 60°, and 80° for sunward directions (*solid lines*), and 100°, 120°, and 150° for anti-Sun direction (*dashed lines*).

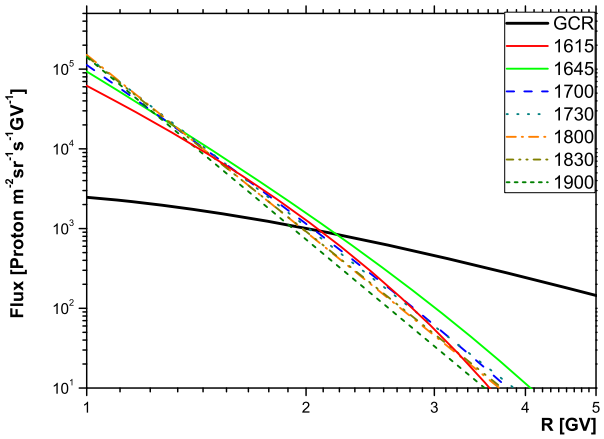

Figure 5 Derived SEP rigidity spectra during GLE 72 on 10 September 2017. Details are given in Table 2. The *black solid line* denotes the GCR particle flux, which corresponds to the time period of the GLE 72 occurrence and includes protons and α-particles, the latter representative also of heavy nuclei. Time [UT] corresponds to the start of the five-minute interval over which the data are integrated.

NM response, while in the analysis we used all the allowed trajectories in the range between the lower rigidity cutoff of the station P_{cut}, *i.e.* the rigidity of the last allowed trajectory, below which all trajectories are forbidden, and the maximum assumed rigidity of SEPs was 20 GV.

The best fit is achieved assuming a modified power-law rigidity spectrum of SEPs and double-Gaussian PAD (see below). For illustration, we plot results with similar fit quality $\mathcal{D}$, while the full details are given in the corresponding tables.

The derived rigidity spectra of the high-energy SEPs during different stages of the event are presented in Figure 5 (details are given in Table 2), assuming a power-law rigidity spectrum and a wide PAD fitted with a double Gaussian (Equations 1 and 3).

The corresponding pitch-angle distributions assuming a double-Gaussian PAD are presented in Figure 6.

An analysis was performed assuming a single-Gaussian PAD. The derived rigidity spectra appear with a similar slope. The corresponding particle flux can be adjusted on the basis of a normalization. This case results in greater residuals $\mathcal{D}$ (for details, see Table 2 and Table 3). Moreover, the two additional criteria for the goodness of fit, *i.e.* a nearly symmetric distribution of the residuals and relative difference between the observed and calculated

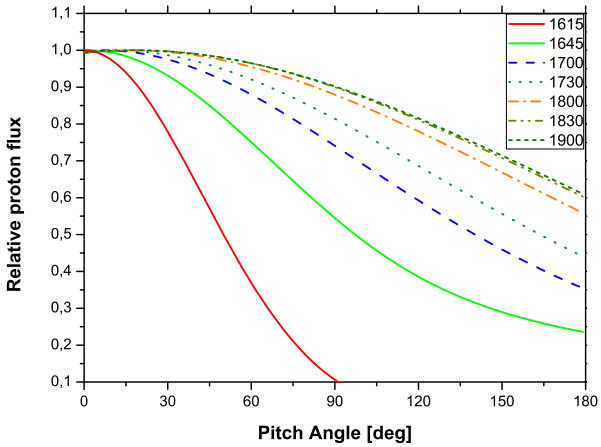

Figure 6 Derived PAD during the GLE 72 on 10 September 2017. Details are given in Table 2. Time [UT] corresponds to the start of the five-minute interval over which the data are integrated.

Table 2 Spectral and angular characteristics of GLE 72 on 10 September 2017, modeled with a modified power-law rigidity spectrum and double-Gaussian PAD.

Integration interval [UT]	J_0 [$m^{-2}\,s^{-1}\,sr^{-1}\,GV^{-1}$]	γ	$\delta\gamma$	σ_1^2 [rad^2]	B	σ_2^2 [rad^2]	Ψ [degrees]	Λ [degrees]	$\mathcal{D}$ [%]
16:15 – 16:20	61900	4.8	0.8	1.1	0.01	0.9	12.0	−56	28.0
16:30 – 16:35	65800	5.5	0.7	3.0	0.20	3.1	9.0	−55	21.0
16:35 – 16:40	77200	5.5	0.4	3.1	0.19	3.1	8.0	−58	18.0
16:45 – 16:50	93500	5.6	0.3	3.2	0.19	3.1	5.0	−56	11.0
17:00 – 17:05	112800	6.4	0.22	5.5	0.20	6.1	2.5	−63	9.2
17:15 – 17:20	138100	7.0	0.0	7.0	0.20	7.2	−2.2	−78	7.7
17:30 – 17:35	145300	7.1	0.0	7.6	0.19	8.1	−4.0	−80	7.8
17:45 – 17:50	151200	7.1	0.0	8.5	0.20	9.5	−5.4	−89	7.6
18:00 – 18:05	151200	7.38	0.0	10.5	0.22	11.5	−6.5	−93	6.1
18:15 – 18:20	148100	7.25	0.0	11.0	0.22	12.0	−7.4	−104	6.8
18:30 – 18:35	145000	7.3	0.0	12.0	0.22	13.0	−8.2	−115	5.9
18:45 – 18:50	138000	7.5	0.0	12.5	0.20	13.0	−14.1	−121	6.2
19:00 – 19:05	141400	7.6	0.0	13.0	0.20	13.0	−11.1	−137	8.0

NM increases to be on the order of 10 – 20%, are not achieved, specifically during the initial phase of the event.

Figure 7 presents the derived SEP rigidity spectra during different stages of the event, assuming a single-Gaussian PAD. Details are given in Table 3.

The corresponding PADs assuming a single Gaussian are presented in Figure 8.

Finally, we tried to fit the global NM network response assuming an exponential rigidity spectrum of SEPs (Equation 2). In this case, the residual $\mathcal{D}$ is considerably greater than in the previous cases: $\mathcal{D}$ is $\approx$ 40 – 50% throughout the whole event.

The accuracy of the modeling is shown by a comparison between the modeled and observed responses for several NMs during the GLE 72 on 10 September 2017 (Figure 9). Note that the quality of the modeling is similar for the other NM stations. The comparison is performed in the case of double-Gaussian PAD (Table 2), while in the case of a single Gaussian

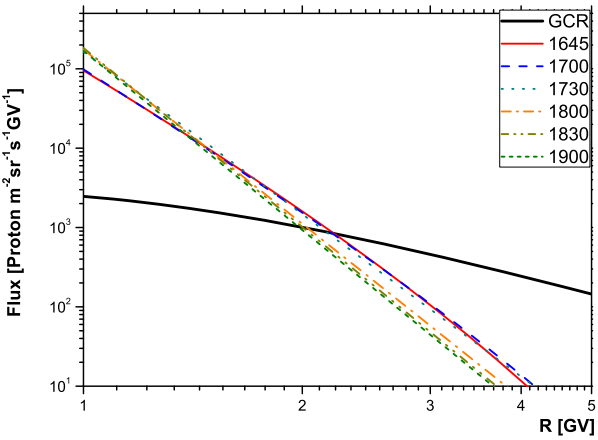

Figure 7 Derived SEP rigidity spectra during the GLE 72 on 10 September 2017. Details are given in Table 3. The *black solid line* denotes the GCR particle flux, which corresponds to the time period of the GLE 72 occurrence and includes protons and α-particles, the latter representative also of heavy nuclei. Time [UT] corresponds to the start of the five-minute interval over which the data are integrated.

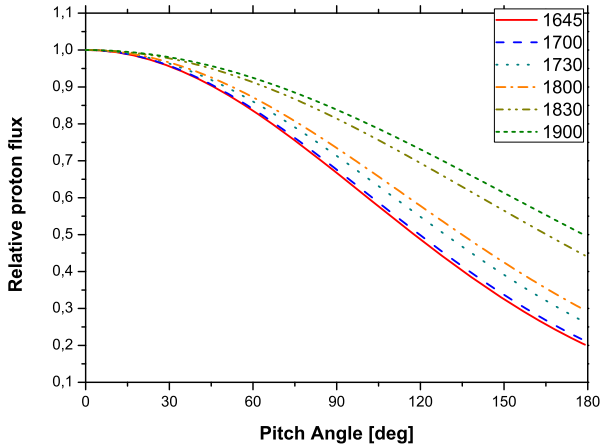

Figure 8 Derived PAD during the GLE 72 on 10 September 2017. Details are given in Table 3. Time [UT] corresponds to the start of the five-minute interval over which the data are integrated.

(Table 3), the difference between modeled and experimental NM responses is considerably greater.

The particle fluence (energy, time, and angle-integrated particle flux) of the GLE 72 is presented in Figure 10 for the early and late phases of the event. As expected, during the early phase of the event, the fluence is dominated by the high-energy part of SEPs. Accordingly, the SEP flux increased at low energies during the late phase of the event.

According to ERNE observations, the related SEPs had an Fe/O abundance ratio below 0.1 at 50 – 100 MeV nucleon^{-1} (Figure 1), which is typical for gradual SEP events (*e.g.* Desai and Burgess, 2008; Desai and Giacalone, 2016, and references therein).

4. Discussion

Here we derived the spectral and anisotropy characteristics of SEPs during the weak GLE 72 event on 10 September 2017 using NM data. According to our analysis, the apparent source position was close to the direction of the IMF lines (Figure 4 and Table 2), the latter being estimated from the 20-minute-averaged *Advanced Composition Explorer* (ACE) spacecraft

Table 3 Derived spectral and angular characteristics of GLE 72 on 10 September 2017, modeled with a modified power-law rigidity spectrum and single Gaussian as PAD.

Integration interval [UT]	J_0 [$m^{-2}\,s^{-1}\,sr^{-1}\,GV^{-1}$]	γ	$\delta\gamma$	σ [rad^2]	Ψ [degrees]	Λ [degrees]	$\mathcal{D}$ [%]
16:45 – 16:50	95500	5.6	0.3	6.1	−3.0	−58	20.0
17:00 – 17:05	98400	5.8	0.22	6.3	−2.5	−64	13.0
17:15 – 17:20	157200	6.5	0.0	7.1	−3.1	−80	12.0
17:30 – 17:35	163700	6.8	0.0	7.8	−5.0	−83	9.5
17:45 – 17:50	170500	6.9	0.0	7.8	−6.5	−92	8.8
18:00 – 18:05	175400	7.2	0.0	8.2	−7.0	−95	8.0
18:15 – 18:20	178200	7.3	0.0	10.0	−5.0	−98	8.0
18:30 – 18:35	183250	7.5	0.0	12.0	−7.5	−105	7.5
18:45 – 18:50	162800	7.4	0.0	12.5	−12.0	−151	6.8
19:00 – 19:05	168100	7.5	0.0	14.0	−15.0	−155	9.4

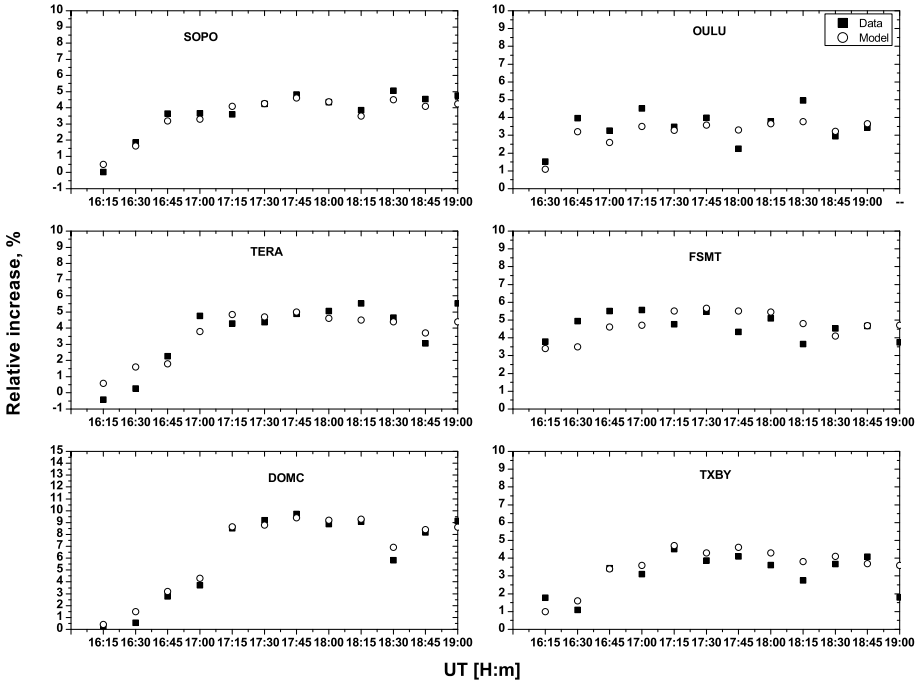

Figure 9 Modeled and observed responses of several NM stations during the GLE 72 on 10 September 2017. The accuracy of the fit for other stations is on the same order.

measurements and explicitly considering the time shift of the field direction at the nose of the Earth's bow shock in a way similar to Mishev, Poluianov, and Usoskin (2017). According to our estimations, the uncertainty of the derived apparent source position is about 10 – 15 degrees, which is consistent with results reported by Bieber *et al.* (2013). This implies that particles were propagating from the Sun close to the nominal Parker spiral.

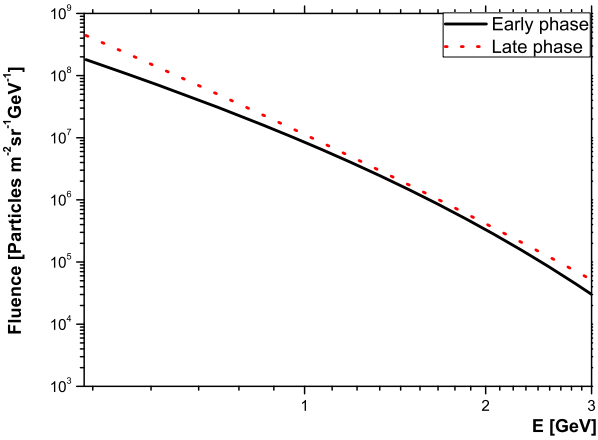

Figure 10 Fluence of high-energy SEP during GLE 72. The SEP fluence for the early phase is angle integrated from 16:15 to 17:15 UT, while the fluence for the late phase is angle integrated from 17:15 to 19:15 UT.

The best fit of the modeled global NM responses was achieved assuming a modified power-law rigidity spectrum (Equation 1) and a wide PAD fitted with a double Gaussian (Equation 3). The SEP spectrum was moderately hard during the event onset and constantly softened throughout the event. A marginal hardening was observed at about 18:15 UT. A steepening of the spectrum with rigidity was observed during the initial phase of the event, which vanished later. Hence, after 17:15 UT, a pure power-law rigidity spectrum was derived. An important anisotropy during the event onset was observed, since there were statistically significant responses at the FSMT and INVK NM stations, but no or an only marginal response at other stations. These NM stations responded to SEP fluxes with narrow pitch angles, as their asymptotic cones were close to the direction of the IMF lines (Figure 4). The angular distribution of the SEPs broadened throughout the event. The timing of the event (first increase at 16:15 with a clear shock formed already at 16:00 in the corona) is consistent with the hypothesis of particle acceleration at a coronal shock driven by the CME. In addition, the ratio Fe/O at 50 – 100 MeV nucleon^{-1} was low, which is typical for a gradual event (Desai and Burgess, 2008; Desai and Giacalone, 2016). However, a more detailed and deep analysis is necessary using all the available data in order to derive relevant information about the SEP acceleration.

This derived PAD could be a result of a focused transport of SEPs. Alternatively, we can speculate that it may be due to a non-standard mode of the particle propagation caused by an interplanetary magnetic-field structure associated with a previous CME (Ruffolo *et al.*, 2006). A detailed analysis and modeling similar to Kocharov *et al.* (2017) is planned for forthcoming work.

5. Conclusions

Here, we have employed an improved method, compared to Mishev, Kocharov, and Usoskin (2014), of an analysis of data from the global NM network: the response of each NM was computed using a yield function corresponding to the exact NM altitude above sea level, and self-consistent and robust optimization similarly to Mishev, Poluianov, and Usoskin (2017), applied for the GLE 72 on 10 September 2017. The dataset included records from 27 NMs distributed over the globe, which encompass a wide range of the particle arrival directions and rigidities.

The method consists of consecutively computing asymptotic directions and the cutoff rigidity of the NM stations, modeling the NM responses, and solving an inverse problem. We modeled the NM responses by applying the Tsyganenko 1989 and IGRF magnetospheric-field models and using a new NM yield function. Herein, the method employs a modified power-law or exponential rigidity spectrum of SEPs and superposition of two Gaussians for PAD.

We have studied several possible cases of spectral and angular distribution of SEPs, namely an exponential or power-law rigidity spectrum, and a single- or double-Gaussian PAD. Hence, we derived the spectral and angular characteristics of GLE particles. The temporal evolution of the spectral and angular characteristics is derived in the course of the event (see the Electronic Supplementary Materials, *i.e.* animations that demonstrate the rigidity spectra and PAD evolution throughout the event). The 10 September 2017 event has revealed a wide PAD that is best fit with a double Gaussian, except for the event-onset phase, when a narrow angular distribution of SEPs is derived. The PAD parameters depict one maximum of SEP flux at/or near zero pitch angle. This is qualitatively consistent with the hypothesis of focused transport (*e.g.* Agueda, Vainio, and Sanahuja, 2012). A fit with a single-Gaussian PAD was excluded during the analysis, specifically during the initial phase of the event (16:30 UT). The two possible fits were compared, and their quality was briefly discussed.

The best fit of the spectral characteristics of SEPs corresponds to a modified power-law rigidity spectrum. The rigidity spectrum during the event onset is harder than that during the late phase of the event. From the derived spectra and PAD alone, it is hardly possible to define an exact scenario of particle acceleration and transport, but the timing of the event as well as the derived ratio Fe/O at $50-100$ MeV nucleon^{-1} is qualitatively consistent with a shock acceleration. This study gives a basis for subsequent studies of SEP acceleration and interplanetary transport.

Acknowledgments This work was supported by the Academy of Finland (project No. 272157, Center of Excellence ReSoLVE and project No. 267186). Operation of the DOMC/DOMB NM was possible due to support of the French–Italian Concordia Station (IPEV program n903 and PNRA Project LTCPAA PNRA14 00091), projects CRIPA and CRIPA-X No. 304435 and Finnish Antarctic Research Program (FINNARP). We acknowledge NMDB and all of the colleagues and PIs from the neutron monitor stations who kindly provided the data used in this analysis, namely Alma Ata, Apatity, Athens, Baksan, Dome C, Dourbes, Forth Smith, Inuvik, Irkutsk, Jang Bogo, Jungfraujoch, Kerguelen, Lomnicky Štit, Magadan, Mawson, Mexico City, Moscow, Nain, Newark, Oulu, Peawanuck, Potchefstroom, Rome, South Pole, Terre Adelie, Thule, Tixie.

Disclosure and Potential Conflicts of Interest The authors declare that they have no conflicts of interest.

References

Agueda, N., Vainio, R., Sanahuja, B.: 2012, A database of > 20 keV electron Green's functions of interplanetary transport at 1 AU. *Astrophys. J. Suppl.* **202**, 18. DOI.

Aschwanden, M.: 2012, GeV particle acceleration in solar flares and ground level enhancement (GLE) events. *Space Sci. Rev.* **171**(1–4), 3. DOI.

Bieber, J.W., Evenson, P.A.: 1995, Spaceship Earth – an optimized network of neutron monitors. In: Taroni, A. (ed.) *Proc. 24th ICRC* **4** 1316. www.researchgate.net/publication/234316437.

Bieber, J.W., Clem, J., Evenson, P., Pyle, R., Sáiz, A., Ruffolo, D.: 2013, Giant ground level enhancement of relativistic solar protons on 2005 January 20. I. Spaceship Earth observations. *Astrophys. J.* **771**(2), 92. DOI.

Bombardieri, D.J., Duldig, M.L., Michael, K.J., Humble, J.E.: 2006, Relativistic proton production during the 2000 July 14 solar event: The case for multiple source mechanisms. *Astrophys. J.* **644**(1), 565. DOI.

Bütikofer, R., Flückiger, E.O., Desorgher, L., Moser, M.R., Pirard, B.: 2009, The solar cosmic ray ground-level enhancements on 20 January 2005 and 13 December 2006. *Adv. Space Res.* **43**(4), 499. DOI.

Caballero-Lopez, R.A.: 2016, An estimation of the yield and response functions for the mini neutron monitor. *J. Geophys. Res.* **121**(8), 7461. DOI.

Cliver, E.W., Kahler, S.W., Reames, D.V.: 2004, Coronal shocks and solar energetic proton events. *Astrophys. J.* **605**, 902. DOI

Cooke, D.J., Humble, J.E., Shea, M.A., Smart, D.F., Lund, N., Rasmussen, I.L., Byrnak, B., Goret, P., Petrou, N.: 1991, On cosmic-ray cutoff terminology. *Nuovo Cimento C* **14**(3), 213. DOI.

Cramp, J.L., Humble, J.E., Duldig, M.L.: 1995, The cosmic ray ground-level enhancement of 24 October 1989. *Proc. Astron. Soc. Austral.* **11**, 28.

Cramp, J.L., Duldig, M.L., Flückiger, E.O., Humble, J.E., Shea, M.A., Smart, D.F.: 1997, The October 22, 1989, solar cosmic enhancement: Ray an analysis the anisotropy spectral characteristics. *J. Geophys. Res.* **102**(A11), 24237. DOI.

Debrunner, H., Flückiger, E.O., Grädel, H., Lockwood, J.A., McGuire, R.E.: 1988, Observations related to the acceleration, injection, and interplanetary propagation of energetic protons during the solar cosmic ray event on February 16, 1984. *J. Geophys. Res.* **93**(A7), 7206.

Dennis, J.E., Schnabel, R.B.: 1996, *Numerical Methods for Unconstrained Optimization and Nonlinear Equations*, Prentice Hall, Englewood Cliffs. 978-0-898713-64-0.

Desai, M.I., Burgess, D.: 2008, Particle acceleration at coronal mass ejection-driven interplanetary shocks and the Earth's bow shock. *J. Geophys. Res.* **113**(A9), A00B006. DOI.

Desai, M., Giacalone, J.: 2016, Large gradual solar energetic particle events. *Living Rev. Solar Phys.* **13**, 3. DOI.

Desorgher, L., Flückiger, E.O., Gurtner, M., Moser, M.R., Bütikofer, R.: 2005, A Geant 4 code for computing the interaction of cosmic rays with the Earth's atmosphere. *Int. J. Mod. Phys. A* **20**, 6802. DOI.

Dorman, L.: 2004, *Cosmic Rays in the Earth's Atmosphere and Underground*, Kluwer, Dordrecht. 1-4020-2071-6.

Drake, J.F., Cassak, P.A., Shay, M.A., Swisdak, M., Quataert, E.: 2009, A magnetic reconnection mechanism for ion acceleration and abundance enhancements in impulsive flares. *Astrophys. J.* **700**, L16. DOI.

Gil, A., Usoskin, I.G., Kovaltsov, G.A., Mishev, A.L., Corti, C., Bindi, V.: 2015, Can we properly model the neutron monitor count rate? *J. Geophys. Res.* **120**, 7172. DOI.

Gopalswamy, N., Xie, H., Yashiro, S., Akiyama, S., Mäkelä, P., Usoskin, I.G.: 2012, Properties of ground level enhancement events and the associated solar eruptions during solar cycle 23. *Space Sci. Rev.* **171**(1–4), 23. DOI.

Gopalswamy, N., Xie, H., Akiyama, S., Mäkelä, P.A., Yashiro, S.: 2014, Major solar eruptions and high-energy particle events during solar cycle 24. *Earth Planets Space* **66**(1), 104. DOI. Cited by 32.

Hatton, C.: 1971, The neutron monitor. In: *Progress in Elementary Particle and Cosmic-ray Physics X*, North-Holland, Amsterdam. Chapter 1.

Himmelblau, D.M.: 1972, *Applied Nonlinear Programming*, McGraw-Hill, New York. 978-0070289215.

Humble, J.E., Duldig, M.L., Smart, D.F., Shea, M.A.: 1991, Detection of 0.5 – 15 GeV solar protons on 29 September 1989 at Australian stations. *Geophys. Res. Lett.* **18**(4), 737. DOI.

Kallenrode, M.-B., Cliver, E.W., Wibberenz, G.: 1992, Composition and azimuthal spread of solar energetic particles from impulsive and gradual flares. *Astrophys. J.* **391**(1), 370.

Kocharov, L., Pohjolainen, S., Mishev, A., Reiner, M.J., Lee, J., Laitinen, T., Didkovsky, L.V., Pizzo, V.J., Kim, R., Klassen, A., Karlicky, M., Cho, K.-S., Gary, D.E., Usoskin, I., Valtonen, E., Vainio, R.: 2017, Investigating the origins of two extreme solar particle events: Proton source profile and associated electromagnetic emissions. *Astrophys. J.* **839**(2), 79. DOI.

Kudela, K., Bučik, R., Bobik, P.: 2008, On transmissivity of low energy cosmic rays in disturbed magnetosphere. *Adv. Space Res.* **42**(7), 1300.

Kudela, K., Usoskin, I.: 2004, On magnetospheric transmissivity of cosmic rays. *Czechoslov. J. Phys.* **54**(2), 239.

Langel, R.A.: 1987, Main field in geomagnetism. In: Jacobs, J.A. (ed.) *Geomagnetism*, Academic Press, London, 249. Chapter 1.

Lara, A., Borgazzi, A., Caballero-Lopez, R.: 2016, Altitude survey of the galactic cosmic ray flux with a mini neutron monitor. *Adv. Space Res.* **58**(7), 1441. DOI.

Lemen, J.R., Title, A.M., Akin, D.J., Boerner, P.F., Chou, C., Drake, J.F., Duncan, D.W., Edwards, C.G., Friedlaender, F.M., Heyman, G.F., Hurlburt, N.E., Katz, N.L., Kushner, G.D., Levay, M., Lindgren, R.W., Mathur, D.P., McFeaters, E.L., Mitchell, S., Rehse, R.A., Schrijver, C.J., Springer, L.A., Stern, R.A., Tarbell, T.D., Wuelser, J.-P., Wolfson, C.J., Yanari, C., Bookbinder, J.A., Cheimets, P.N., Caldwell, D., Deluca, E.E., Gates, R., Golub, L., Park, S., Podgorski, W.A., Bush, R.I., Scherrer, P.H., Gummin, M.A., Smith, P., Auker, G., Jerram, P., Pool, P., Soufli, R., Windt, D.L., Beardsley, S., Clapp, M., Lang, J., Waltham, N.: 2012, The Atmospheric Imaging Assembly (AIA) on the Solar Dynamics Observatory (SDO). *Solar Phys.* **275**(1–2), 17. DOI.

Levenberg, K.: 1944, A method for the solution of certain non-linear problems in least squares. *Q. Appl. Math.* **2**, 164.

Li, G., Moore, R., Mewaldt, R.A., Zhao, L., Labrador, A.W.: 2012, A twin-CME scenario for ground level enhancement events. *Space Sci. Rev.* **171**(1–4), 141.

Lockwood, J.A., Debrunner, H., Flückiger, E.O.: 1990, Indications for diffusive coronal shock acceleration of protons in selected solar cosmic ray events. *J. Geophys. Res.* **95**(A4), 4187.

Mangeard, P.-S., Ruffolo, D., Sáiz, A., Nuntiyakul, W., Bieber, J.W., Clem, J., Evenson, P., Pyle, R., Duldig, M.L., Humble, J.E.: 2016, Dependence of the neutron monitor count rate and time delay distribution on the rigidity spectrum of primary cosmic rays. *J. Geophys. Res.* **121**(12), 11620. DOI.

Marquardt, D.: 1963, An algorithm for least-squares estimation of nonlinear parameters. *SIAM J. Appl. Math.* **11**(2), 431.

Mavrodiev, S.C., Mishev, A.L., Stamenov, J.N.: 2004, A method for energy estimation and mass composition determination of primary cosmic rays at the Chacaltaya observation level based on the atmospheric Cherenkov light technique. *Nucl. Instrum. Methods Phys. Res., Sect. A, Accel. Spectrom. Detect. Assoc. Equip.* **530**(3), 359. DOI.

Mavromichalaki, H., Papaioannou, A., Plainaki, C., Sarlanis, C., Souvatzoglou, G., Gerontidou, M., Papailiou, M., Eroshenko, E., Belov, A., Yanke, V., Flückiger, E.O., Bütikofer, R., Parisi, M., Storini, M., Klein, K.-L., Fuller, N., Steigies, C.T., Rother, O.M., Heber, B., Wimmer-Schweingruber, R.F., Kudela, K., Strharsky, I., Langer, R., Usoskin, I., Ibragimov, A., Chilingaryan, A., Hovsepyan, G., Reymers, A., Yeghikyan, A., Kryakunova, O., Dryn, E., Nikolayevskiy, N., Dorman, L., Pustil'Nik, L.: 2011, Applications and usage of the real-time neutron monitor database. *Adv. Space Res.* **47**, 2210.

Mishev, A.L., Kocharov, L.G., Usoskin, I.G.: 2014, Analysis of the ground level enhancement on 17 May 2012 using data from the global neutron monitor network. *J. Geophys. Res.* **119**, 670. DOI.

Mishev, A., Poluianov, S., Usoskin, I.: 2017, Assessment of spectral and angular characteristics of sub-GLE events using the global neutron monitor network. *J. Space Weather Space Clim.* **7**, A28. DOI.

Mishev, A., Usoskin, I.: 2016a, Analysis of the ground level enhancements on 14 July 2000 and on 13 December 2006 using neutron monitor data. *Solar Phys.* **291**, 1225. DOI.

Mishev, A., Usoskin, I.: 2016b, Erratum to: Analysis of the ground level enhancements on 14 July 2000 and on 13 December 2006 using neutron monitor data. *Solar Phys.* **291**, 1579. DOI.

Mishev, A., Usoskin, I., Kocharov, L.: 2017, Using global neutron monitor network data for GLE analysis: Recent results. In: *Proc. 35th ICRC*, 147. DOI.

Mishev, A., Usoskin, I., Kovaltsov, G.: 2013, Neutron monitor yield function: New improved computations. *J. Geophys. Res.* **118**, 2783. DOI.

Mishev, A., Usoskin, I., Kovaltsov, G.: 2016, New neutron monitor yield function computed at several altitudes above the sea level: Application for GLE analysis. In: *Proc. 34th ICRC*, 159. DOI.

Moraal, H., McCracken, K.G.: 2012, The time structure of ground level enhancements in solar cycle 23. *Space Sci. Rev.* **171**(1–4), 85.

Nevalainen, J., Usoskin, I., Mishev, A.: 2013, Eccentric dipole approximation of the geomagnetic field: Application to cosmic ray computations. *Adv. Space Res.* **52**(1), 22. DOI.

Papaioannou, A., Souvatzoglou, G., Paschalis, P., Gerontidou, M., Mavromichalaki, H.: 2014, The first ground-level enhancement of solar cycle 24 on 17 May 2012 and its real-time detection. *Solar Phys.* **289**, 423. DOI.

Reames, D.V.: 1999, Particle acceleration at the Sun and in the heliosphere. *Space Sci. Rev.* **90**(3–4), 413.

Reames, D.V.: 2013, The two sources of solar energetic particles. *Space Sci. Rev.* **175**(1–4), 53. DOI.

Ruffolo, D., Tooprakai, P., Rujiwarodom, M., Khumlumlert, T., Wechakama, M., Bieber, J.W., Evenson, P.A., Pyle, K.R.: 2006, Relativistic solar protons on 1989 October 22: Injection and transport along both legs of a closed interplanetary magnetic loop. *Astrophys. J.* **639**(2), 1186. DOI.

Shea, M.A., Smart, D.F.: 1982, Possible evidence for a rigidity-dependent release of relativistic protons from the solar corona. *Space Sci. Rev.* **32**, 251.

Shea, M.A., Smart, D.F.: 1990, A summary of major solar proton events. *Solar Phys.* **127**, 297. DOI. ADS.

Simpson, J., Fonger, W., Treiman, S.: 1953, Cosmic radiation intensity-time variation and their origin. I. Neutron intensity variation method and meteorological factors. *Phys. Rev.* **90**, 934.

Souvatzoglou, G., Papaioannou, A., Mavromichalaki, H., Dimitroulakos, J., Sarlanis, C.: 2014, Optimizing the real-time ground level enhancement alert system based on neutron monitor measurements: Introducing *GLE Alert Plus*. *Space Weather* **12**(11), 633. DOI.

Stoker, P.H., Dorman, L.I., Clem, J.M.: 2000, Neutron monitor design improvements. *Space Sci. Rev.* **93**(1–2), 361.

Tikhonov, A.N., Goncharsky, A.V., Stepanov, V.V., Yagola, A.G.: 1995, *Numerical Methods for Solving Ill-Posed Problems*, Kluwer, Dordrecht. 978-90-481-4583-6.

Tsyganenko, N.A.: 1989, A magnetospheric magnetic field model with a warped tail current sheet. *Planet. Space Sci.* **37**(1), 5.

Tylka, A., Dietrich, W.: 2009, A new and comprehensive analysis of proton spectra in ground-level enhanced (GLE) solar particle events. In: *Proc. of 31th ICRC*, 0273.

Vainio, R., Valtonen, E., Heber, B., Malandraki, O.E., Papaioannou, A., Klein, K.-L., Afanasiev, A., Agueda, N., Aurass, H., Battarbee, M., Braune, S., Dröge, W., Ganse, U., Hamadache, C., Heynderickx, D., Huttunen-Heikinmaa, K., Kiener, J., Kilian, P., Kopp, A., Kouloumvakos, A., Maisala, S., Mishev, A., Miteva, R., Nindos, A., Oittinen, T., Raukunen, O., Riihonen, E., Rodríguez-Gasén, R., Saloniemi, O., Sanahuja, B., Scherer, R., Spanier, F., Tatischeff, V., Tziotziou, K., Usoskin, I.G., Vilmer, N.: 2013, The first SEPserver event catalogue ∼68-MeV solar proton events observed at 1 AU in 1996 – 2010. *J. Space Weather Space Clim.* **3**, A12. DOI.

Vainio, R., Raukunen, O., Tylka, A.J., Dietrich, W.F., Afanasiev, A.: 2017, Why is solar cycle 24 an inefficient producer of high-energy particle events? *Astron. Astrophys.* **604**, A47. DOI.

Vashenyuk, E.V., Balabin, Y.V., Perez-Peraza, J., Gallegos-Cruz, A., Miroshnichenko, L.I.: 2006, Some features of the sources of relativistic particles at the Sun in the solar cycles 21 – 23. *Adv. Space Res.* **38**(3), 411.

Vashenyuk, E.V., Balabin, Y.V., Gvozdevsky, B.B., Schur, L.I.: 2008, Characteristics of relativistic solar cosmic rays during the event of December 13, 2006. *Geomagn. Aeron.* **48**(2), 149.